Slow mode waves and quasi-periodic upflows in the multi-temperature solar corona as seen by the SDO

V. M. Uritsky[1,2], J. M. Davila[1], N. M. Viall[1], and L. Ofman[2]

[1]NASA/GSFC, Greenbelt MD
[2] Catholic University of America, Washington DC

Talk plan

1. Propagating disturbances (PDs) in coronal loops: brief review
2. Surfing transform (ST) technique and SDO AIA data (AR 11082)
3. Measuring temperature-dependent propagation speeds using ST
4. Spatial dependence of PD in the studied fan loop system
5. Statistical analysis of velocity ratios vs sound wave ratios
6. Examples of low-altitude PDs: downward plasma flows ?
7. Conclusions and open problems

Slow magnetosponic waves in coronal plumes
(L. Ofman et al., ApJ 1999; DeForest & Gurman 1998)

(a)

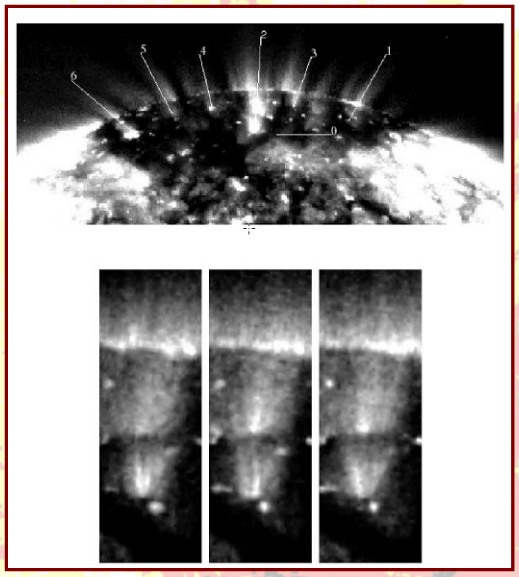

(b)

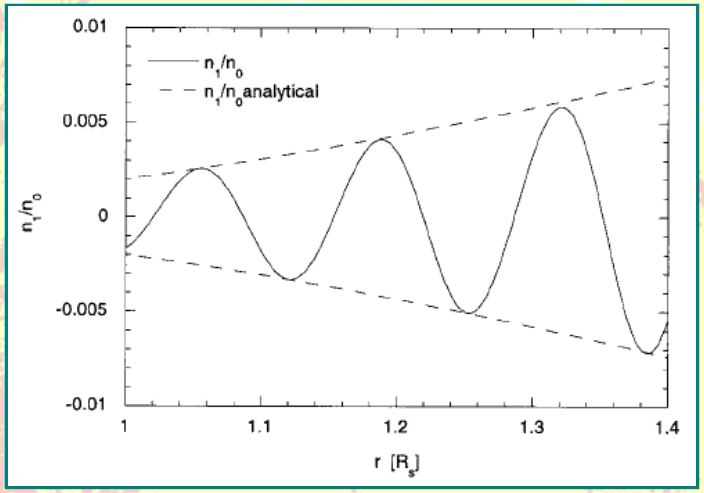

(c)

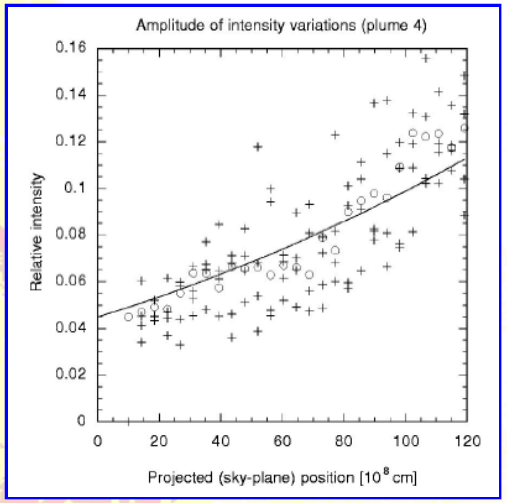

(a) Polar plumes over the south pole of the Sun as seen in the EIT 171 A;
(b) Radial dependence of the relative density fluctuation (solid line) obtained from a numerical solution of MHD equations;
(c) Wave amplitude (relative to the background intensity) dependence on the height, solid line shows the analytical slow mode fit.

Slow magnetisonic waves in coronal loops
(T.J.Wang et at, ApJ 2009)

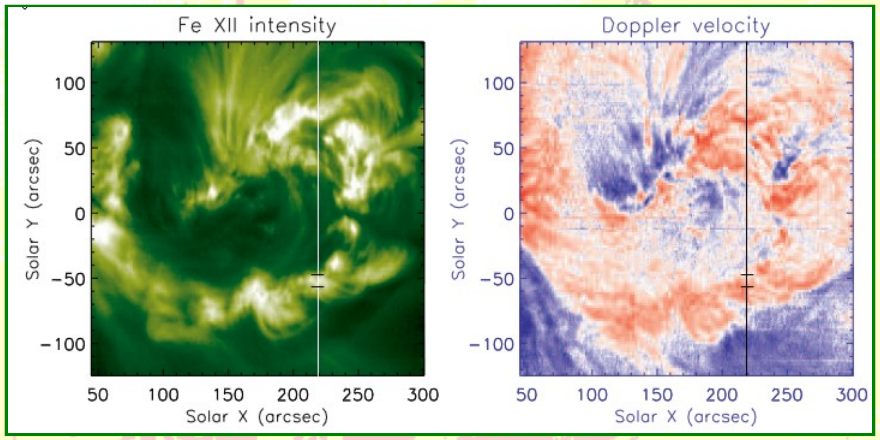

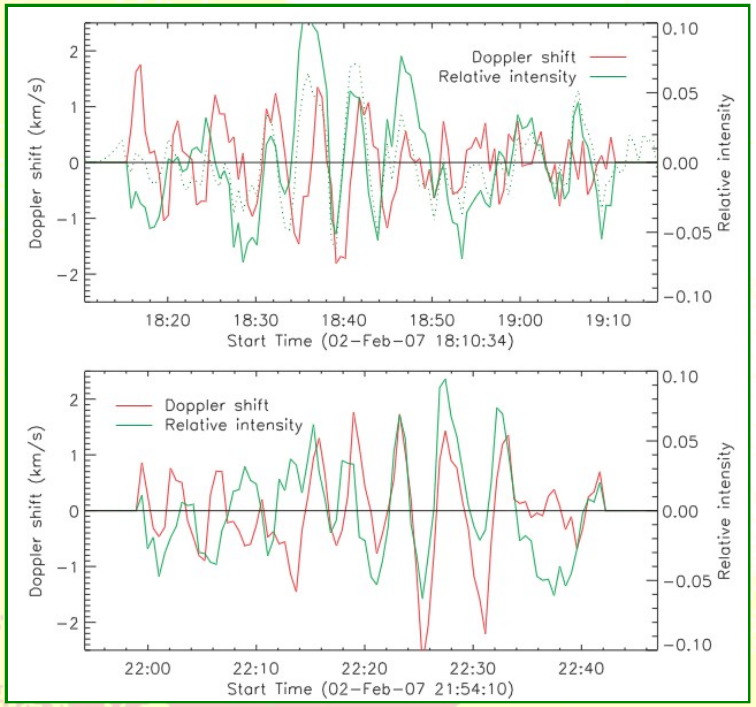

Left: intensity map in the Fe XII 195 A line from Hinode/ EIS. Right: Doppler velocity measurements.

In-phase relation between Doppler shift and intensity oscillations

Waves or periodic upflows?
(H. Tian et al., ApJ 2011)

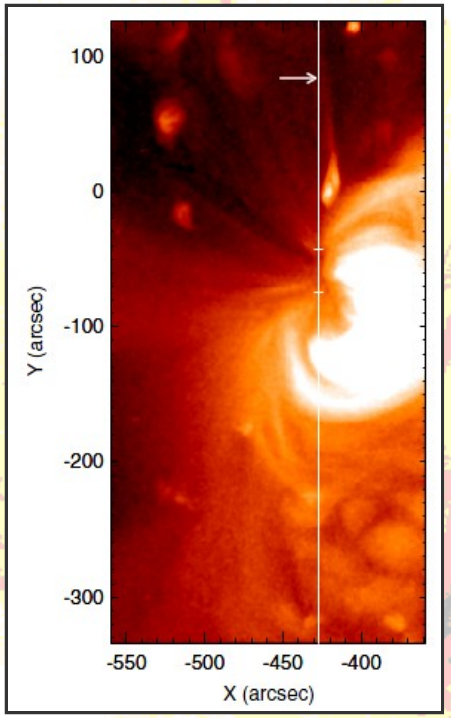

Hinode / XRT image of the studied AR NOAA 10942

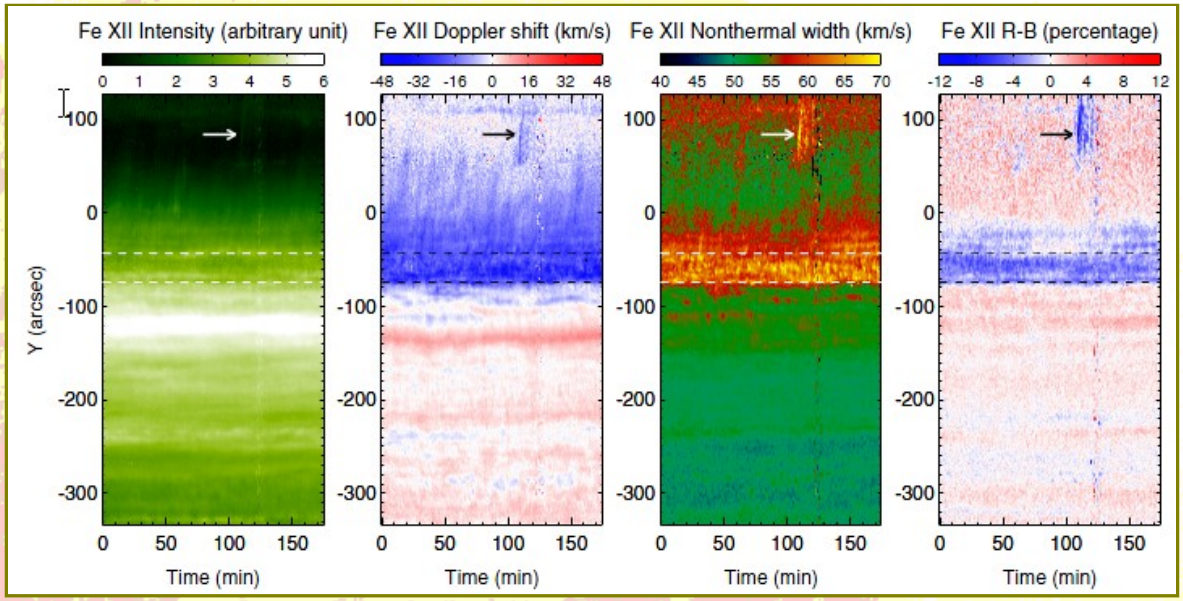

Temporal evolution of the line peak intensity, Doppler shift, non-thermal width, and R–B asymmetry of the Fe XII195 A line. The arrow points to an isolated strong upflow event.

GEOPHYSICAL RESEARCH LETTERS, VOL. 36, L21103, doi:10.1029/2009GL040777, 2009

Longitudinally propagating arc wave in the pre-onset optical aurora

V. M. Uritsky,[1] J. Liang,[1] E. Donovan,[1] E. Spanswick,[1] D. Knudsen,[1] W. Liu,[2] J. Bonnell,[3] and K. H. Glassmeier[4,5]

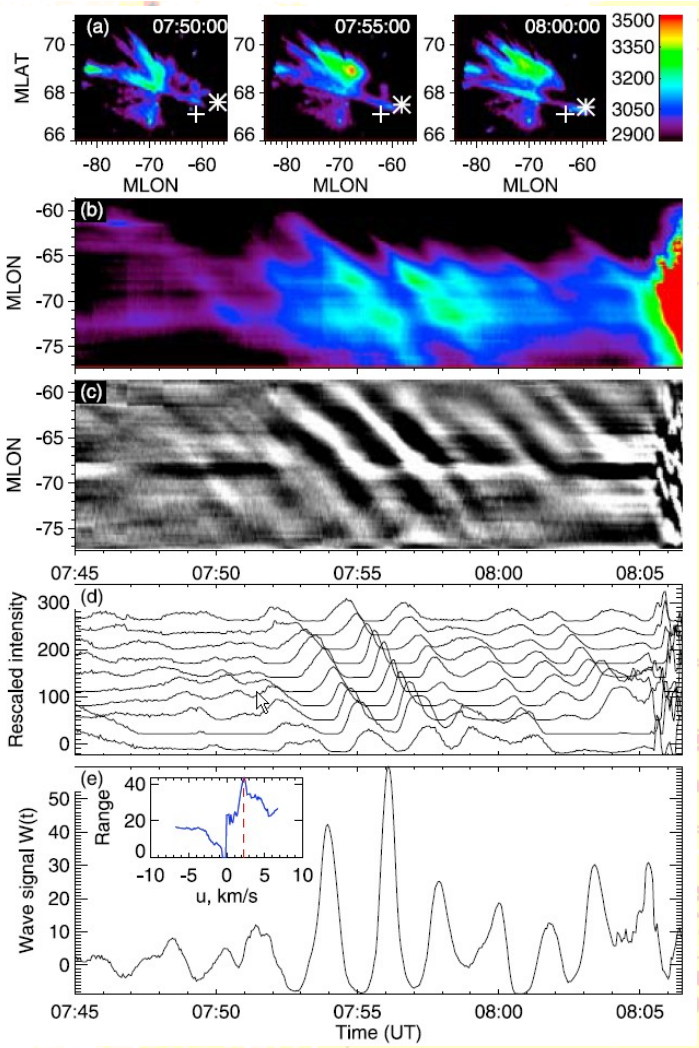

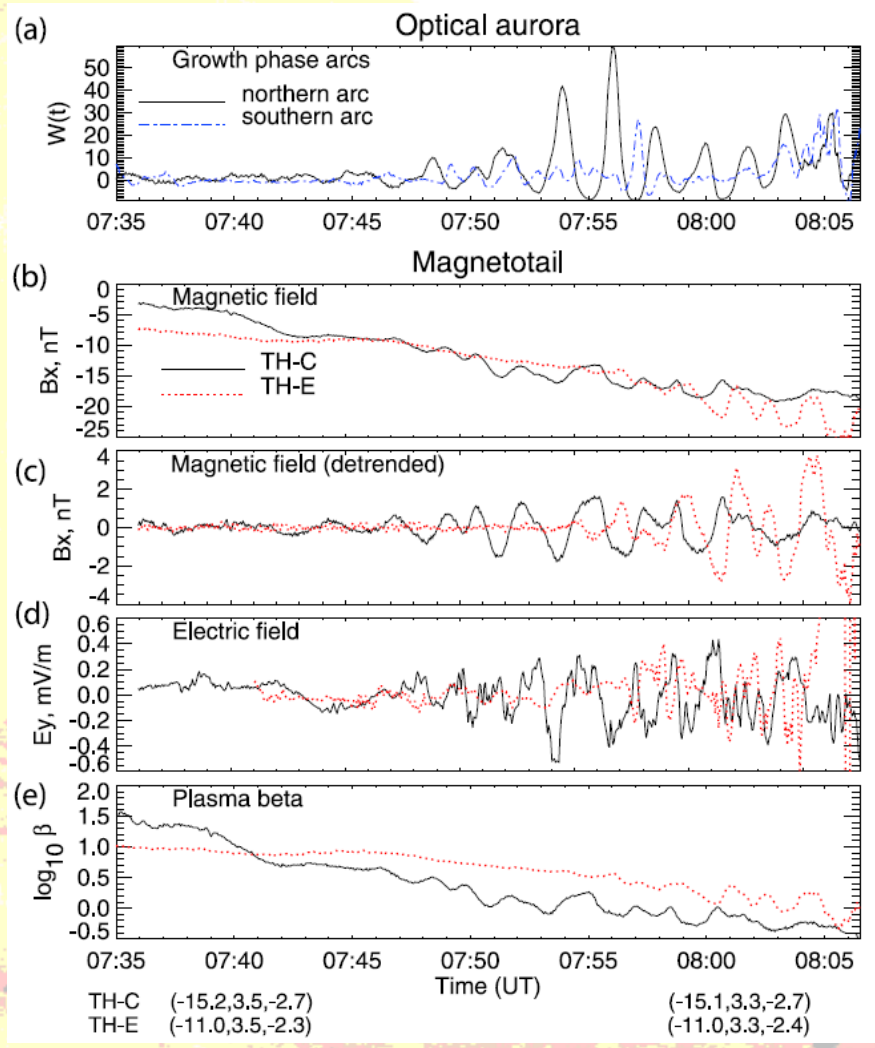

Surfing transform (ST)

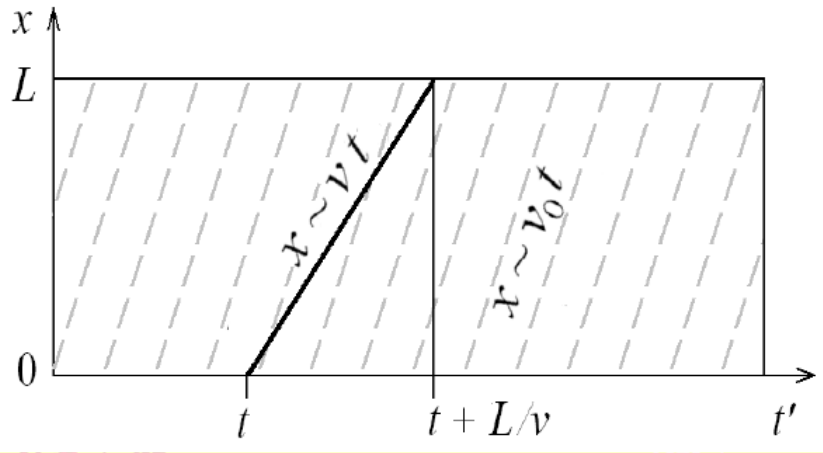

$$a_S(t,v) = \frac{v}{L} \int_t^{t+L/v} a(x = x_S, t')dt'.$$

t — starting time

$x_S = v \times (t' - t)$ — averaging path

L — propagated distance,

v — surfing velocity

ST of 1-dimensional harmonic wave oscillation

$$a_S(t,v) = \frac{v}{L}\int_t^{t+L/v} a_0 \cos\left(k_0 v \times (t'-t) - \omega_0 t'\right) dt'$$

$$= \frac{a_0 v}{L(k_0 v - \omega_0)} \left\{\sin\left([k_0 v - \omega_0]\,[t + L/v] - k_0 v t\right) - \sin\left([k_0 v - \omega_0]\,t - k_0 v t\right)\right\}$$

$$= a_0 \frac{\sin(\xi)}{\xi} \cos(\omega_0 t + \xi) \quad \text{with } \xi = \frac{L(k_0 v - \omega_0)}{2v},$$

[used the identity $\sin(\alpha) - \sin(\beta) = 2\sin(\frac{\alpha-\beta}{2})\cos(\frac{\alpha+\beta}{2})$]

dispersionless case

phase speed $v_0 = \omega_0/k_0$

velocity detuning parameter $\xi = L\omega_0(v - v_0)/(2vv_0)$

$v \to v_0$

$\xi \to 0$

$a_S(t,v) \to a_0 = \max(a_S)$ velocity resonance

ST spectrum

$$P_S(f,v) = \frac{v}{L}\left|\int_{-\infty}^{\infty}\int_{t}^{t+L/v} a(v\times(t'-t),t')e^{-i2\pi ft}dt'dt\right|^2$$

Velocity spectrogram

$$P_S(v, f = f_0) = P_0\ \mathrm{sinc}^2(L\omega_0(v-v_0)/(2vv_0))$$

reaches maximum at $v = v_0$

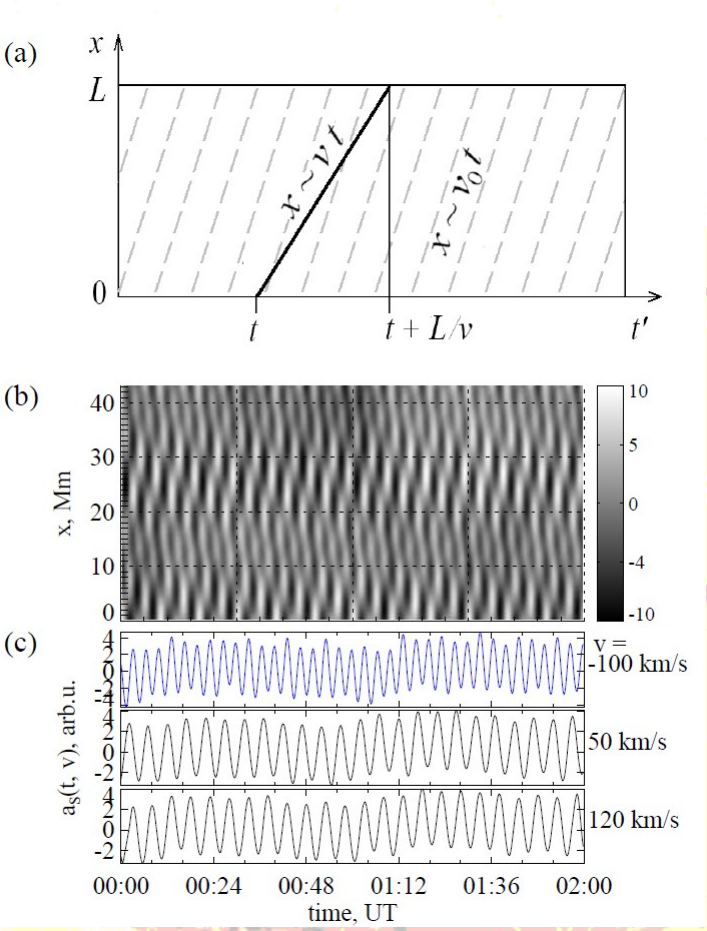

$$a(x,t) = \sum_{i=1}^{3} a_0 \cos\left(k_i x - \omega_i t\right) + \sigma\zeta_{x,t}$$

$$[\omega_1, \omega_2, \omega_3]/(2\pi) = [5.00, 3.33, 3.33] \text{ mHz}$$

$$[v_1, v_2, v_3] = [-100, 50, 120] \text{ km/s}$$

$$k_i = \omega_i / v_i.$$

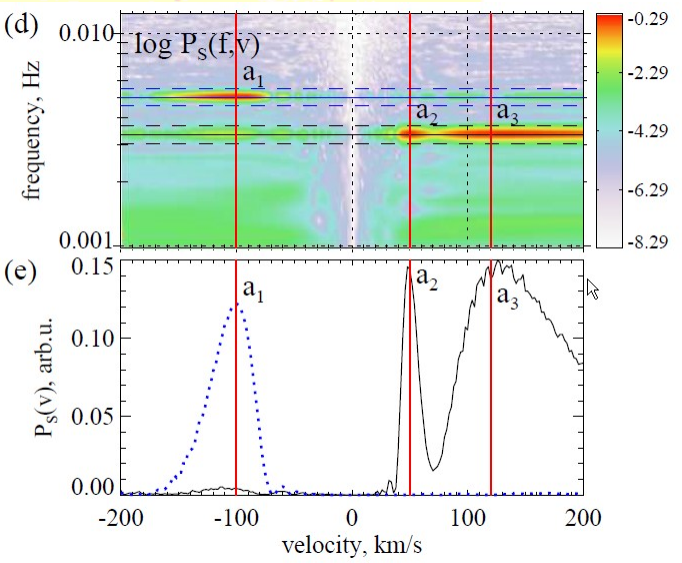

(a) Extraction of the ST signal from a position-time plot. Dashed lines show the fronts of a periodic PD described with phase speed v0, solid line is the averaging path defined by the surfing speed v and the starting time t, L is the size of the studied region. (b) Position-time plot of the simulated noisy wave signal defined by Eq. (5). (c) Surfing signals obtained using three values of v matching the phase speeds of the wave components. (d) ST spectrum computed using 400 ST signals covering the velocity range −200 … 200 km/s. (e) Velocity spectrograms representing horizontal sections of the ST spectrum at f_0 = 5.00 mHz (dotted blue line) and f_0 = 3.3 mHz (solid black line).

NOAA AR 11082

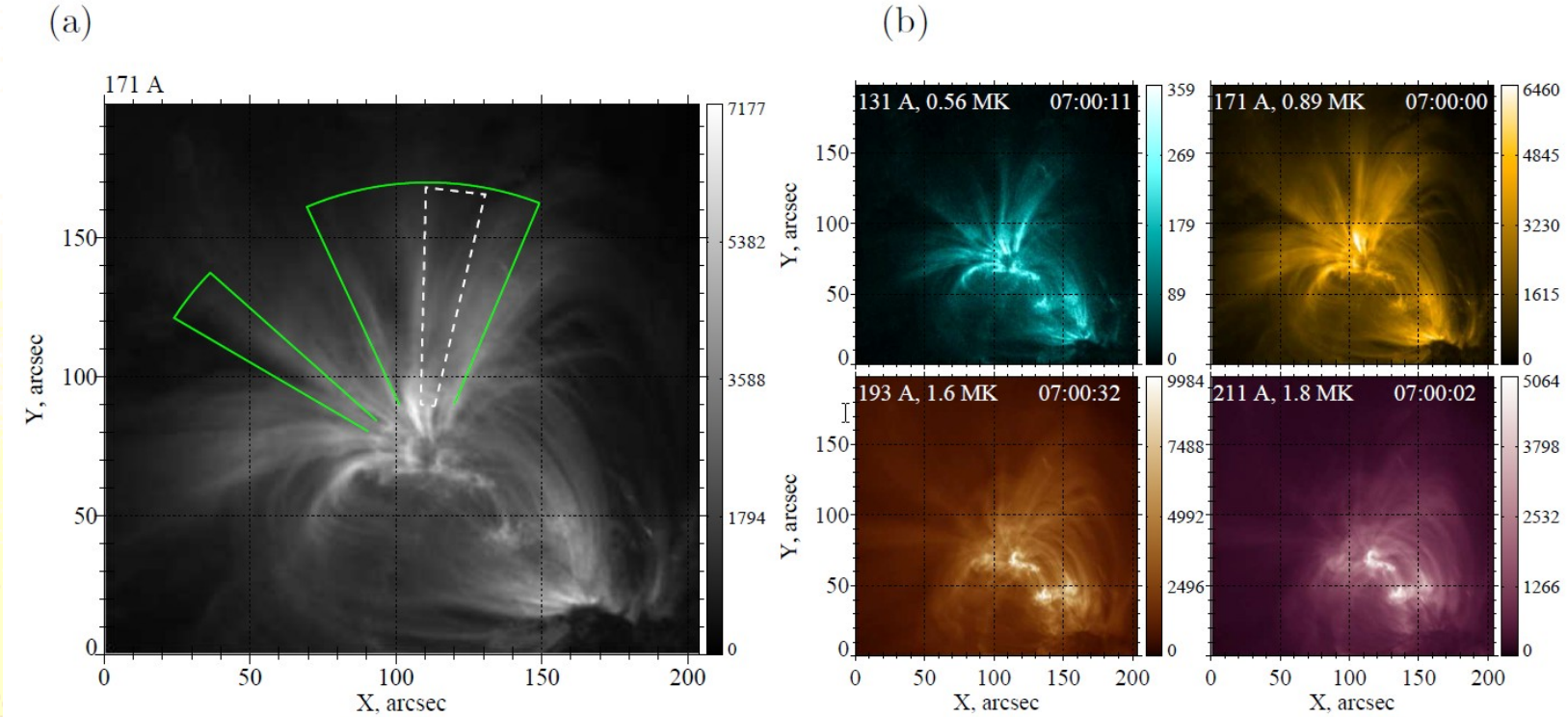

(a) A snapshot of the active region NOAA AR 11082 as seen in the 171 A SDO AIA channel at 7:00:00 UT. The dashed white lines show the domain of the most consistent PD activity. The solid green lines outline the region of detectable slow wave activity. (b) Multi-spectral AIA images of the same region obtained at around the same time; temperatures values are for the peaks of the response functions based on the 2013 release of the CHIANTI atomic database (Dere et al. 1997; Landi et al. 2013).

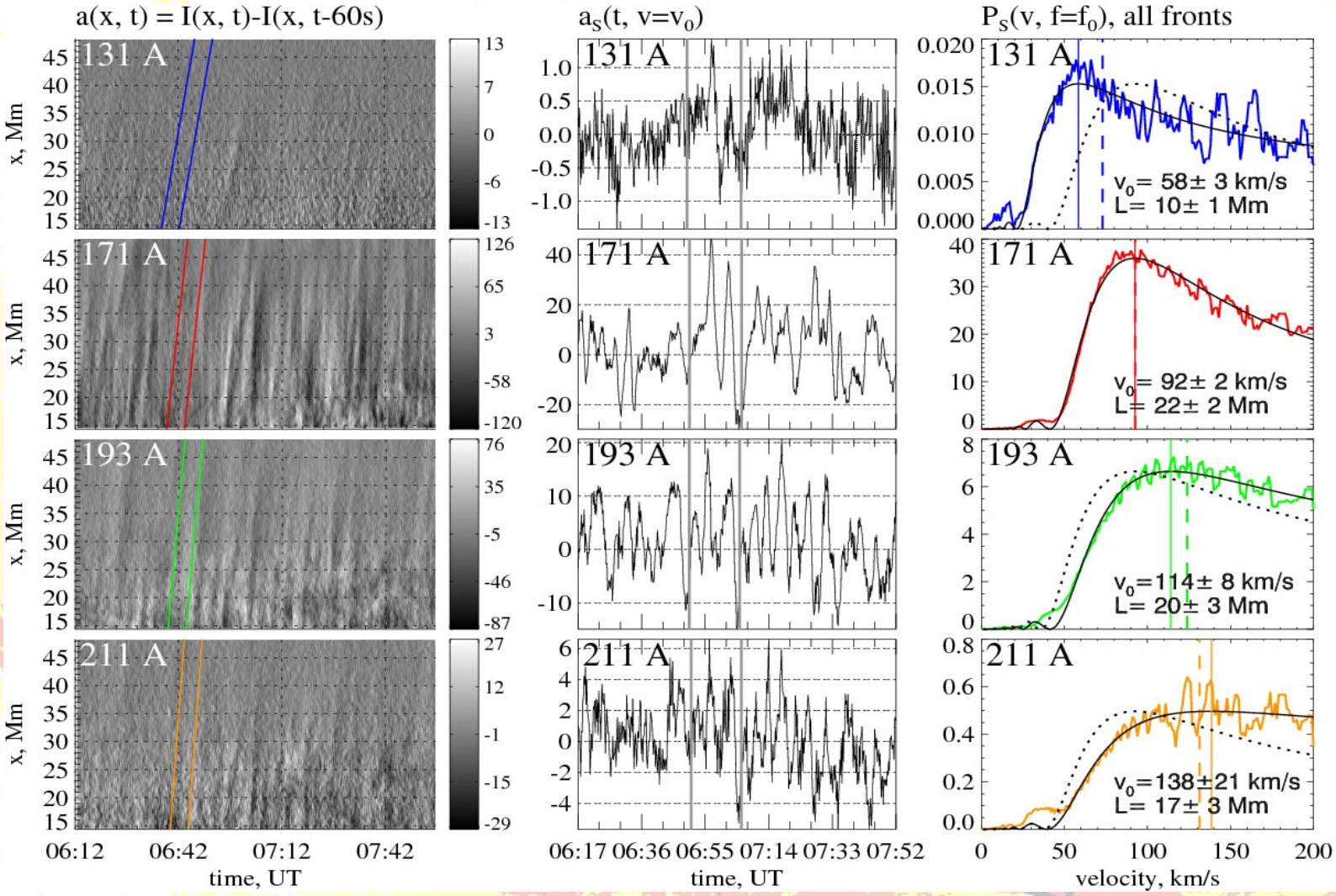
a(x, t) = I(x, t)-I(x, t-60s)
$a_S(t, v=v_0)$
$P_S(v, f=f_0)$, all fronts
131 A
171 A
193 A
211 A
x, Mm
time, UT
velocity, km/s
v_0= 58± 3 km/s
L= 10± 1 Mm
v_0= 92± 2 km/s
L= 22± 2 Mm
v_0=114± 8 km/s
L= 20± 3 Mm
v_0=138±21 km/s
L= 17± 3 Mm

v~ 90-110 km/s: consistent with previous measurements

Table 8.1: Observations of slow-mode (acoustic) waves in coronal structures. N is the number of analyzed events.

Observer	N	Frequency or wavelength	Wave speed v [km/s]	Instrument	Morphology
DeForest & Gurman (1998)	1	171 Å	$\approx 75 - 150$	SoHO/EIT	polar plumes
Berghmans & Clette (1999)	3	195 Å	$\approx 75 - 200$	SoHO/EIT	quasi-open field lines
De Moortel et al. (2000b)	1	171 Å	$\approx 70 - 165$	TRACE	fan loop
De Moortel et al. (2002a)	38	171 Å	122 ± 43	TRACE	fan loop
De Moortel et al. (2002b)	4	195 Å	150 ± 25	TRACE	fan loop
De Moortel et al. (2002c)	38	171 Å	122 ± 43	TRACE	fan loop
Robbrecht et al. (2001)	4	171, 195 Å	$\approx 65 - 150$	EIT, TRACE	fan loops
Berghmans et al. (2001)	1	171, 195 Å	...	EIT, TRACE	open & closed field lines
Sakurai et al. (2002)	1	5303 Å	≈ 100	Norikura	polar plumes
King et al. (2003)	1	171, 195 Å	...	TRACE	fan loops
Marsh et al. (2003)	1	171, 368 Å	$\approx 50 - 195$	CDS, TRACE	quasi-open field lines

from M. Aschwanden, *Physics of Solar Corona* (Springer 2005)

3-5 min period: p-mode oscillation ?

Velocity ratios measured for the entire wave event and two selected fronts, as compared to the predicted sound speed ratios.

Wavelength	All fronts	Selected fronts	Predicted
131 Å	0.63 ± 0.03	0.86 ± 0.04	0.79
171 Å	1	1	1
193 Å	1.23 ± 0.08	1.31 ± 0.06	1.34
211 Å	1.50 ± 0.23	1.50 ± 0.15	1.42

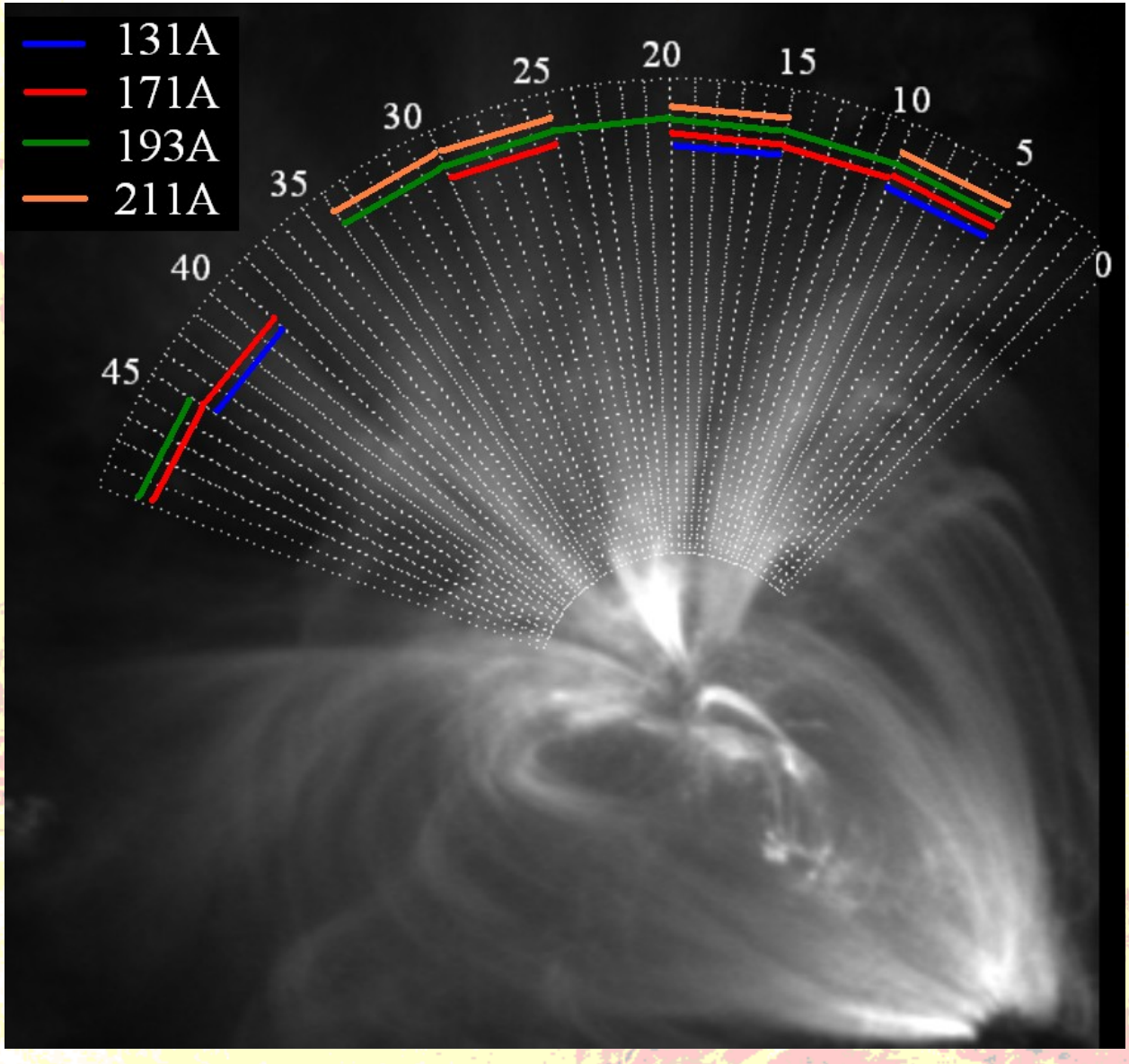
131A
171A
193A
211A
0
5
10
15
20
25
30
35
40
45

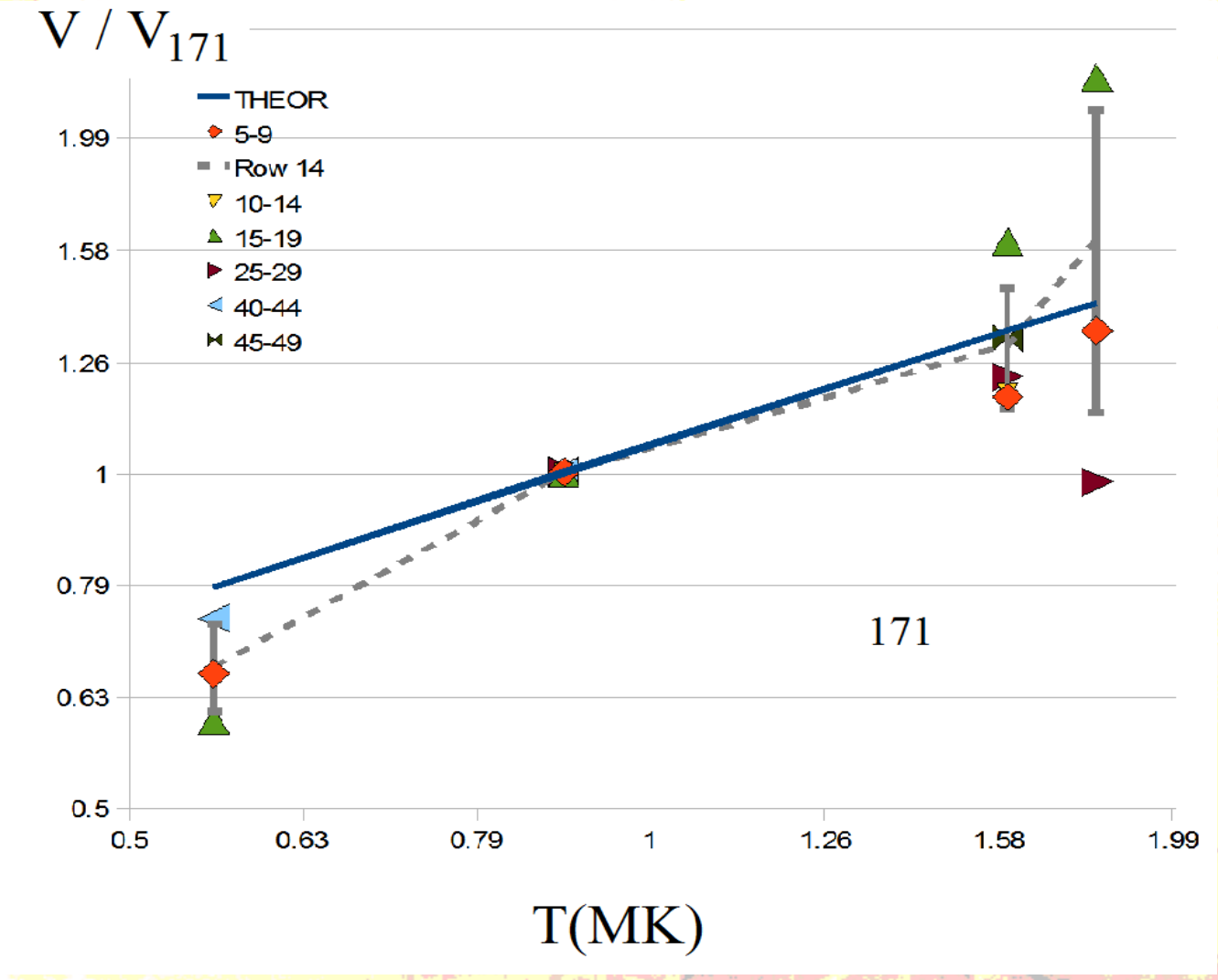
V / V171
THEOR
5-9
Row 14
10-14
15-19
25-29
40-44
45-49
1.99
1.58
1.26
1
0.79
0.63
0.5
0.5
0.63
0.79
1
1.26
1.58
1.99
171
T(MK)

Example of downwardly propagating PDs

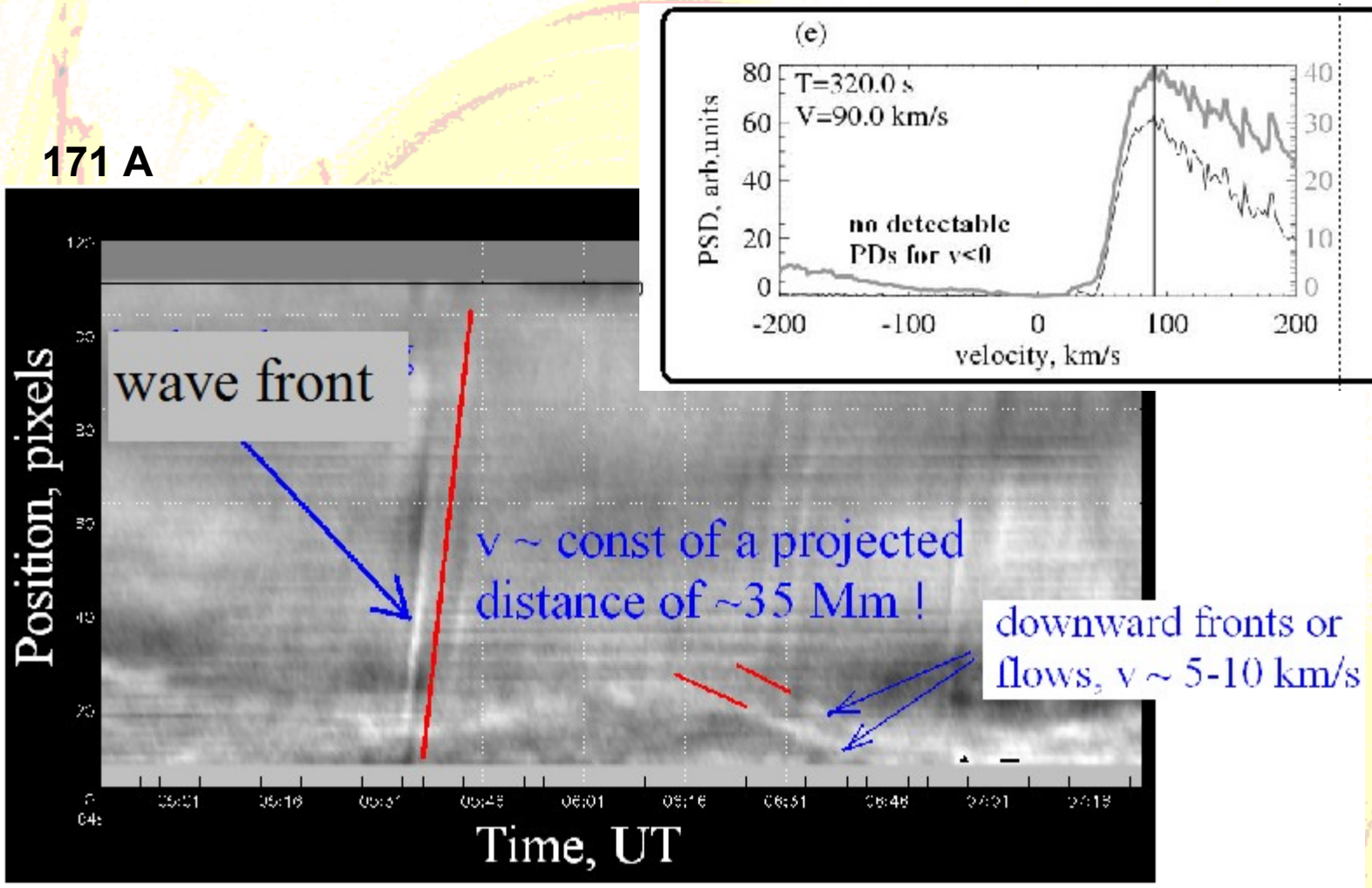

Conclusions

(1) We have presented a new methodology for measuring parameters of PDs in multi-temperature coronal images based on the ST technique.

(2) The developed methodology has been applied to the analysis of PDs in coronal fan loops in AR 11082 across a range of temperatures covered by four SDO AIA channels.

(3) We found that traveling velocity of the disturbances propagating along the studied system of loops obeys an approximate square root temperature dependence predicted for slow mode magneto-acoustic waves which seems to be the dominating wave mode in the studied loop structures.

(4) Our slow-mode observations extend recent findings by Kiddie et al (Solar Pys 2012) by demonstrating temperature-dependent PD activity simultaneously in four AIA channels in a non-sunspot active region.

(5) Closer to the base of the corona, we observed occasional downwardly directed PDs with a significantly lower velocity, possibly associated with bulk plasma flows.

(6) It remains to be clarified whether or not the magnetosonic wave activity at higher altitudes is driven by (partially undetected) fast plasma flows at the base of the corona as has been proposed by some authors (Tian et al. 2011b,a; Warren et al. 2011; Ugarte-Urra & Warren 2011; Su et al. 2012; Ofman et al. 2012).

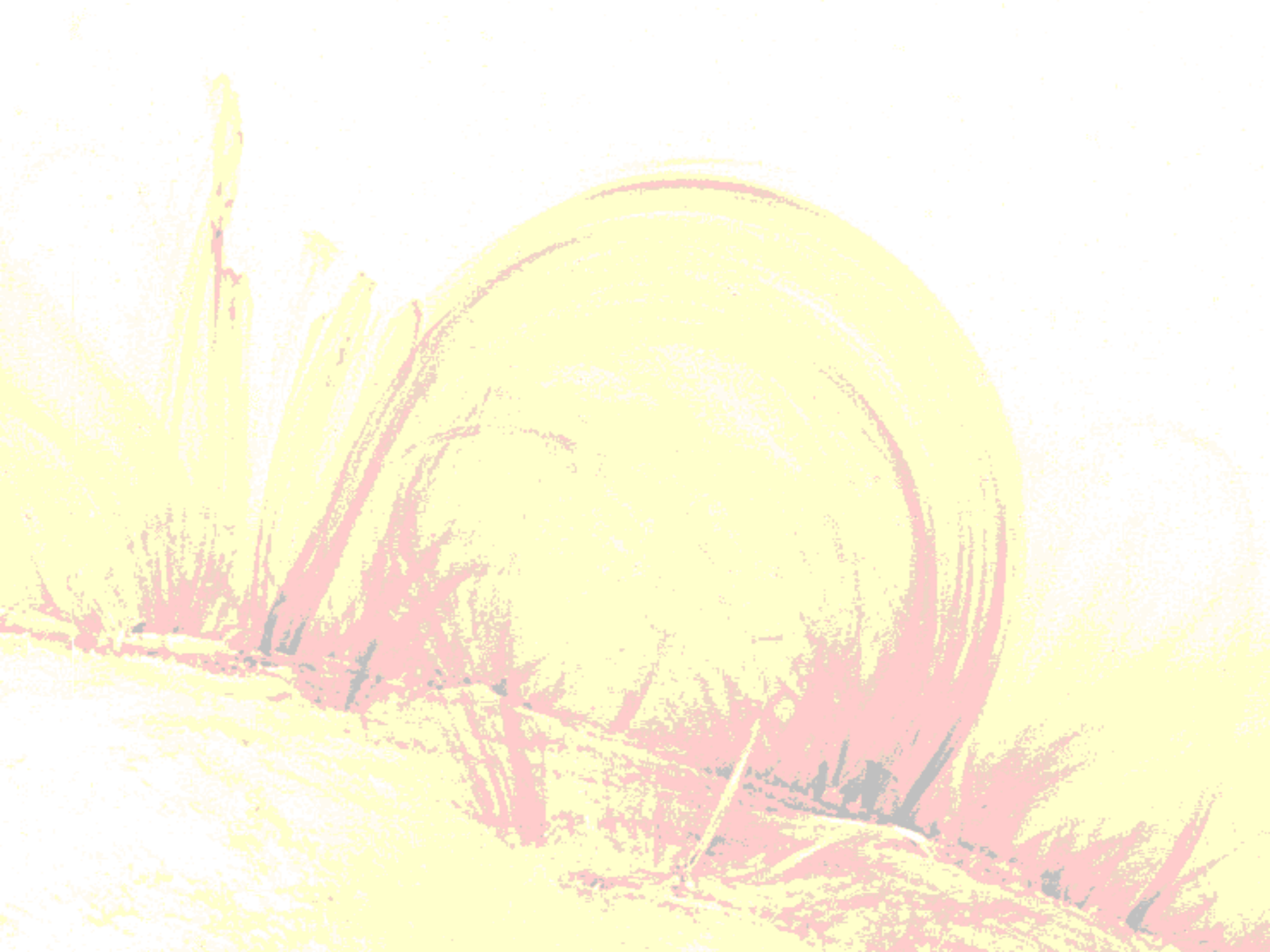

The wave - flow dilemma

- **Waves**: Moortel et al. 2000; Nakariakov et al. 2000; Ofman et al. 1999, 2000; Marsh et al. 2009; Wang et al. 2009b,a; Prasad et al. 2012; Kiddie et al. 2012, …
- **Flows**: Tian et al. 2011b,a; Warren et al. 2011; Ugarte-Urra & Warren 2011; Su et al. 2012; …
- **Wave-flow interaction**: De Pontieu and McIntosh, 2010; Nishizuka & Hara 2011; Ofman et al. 2012; ...
- **Counter-propagating flows**: Kamio et al. 2011; Young et al. 2012, ...

local sound speed

$$c_s^2 = \gamma\, p/\rho \propto T$$

γ – adiabatic index

p – kinetic pressure

ρ – mass density

T – temperature

velocity-temperature scaling

$$v \propto T^{1/2}$$

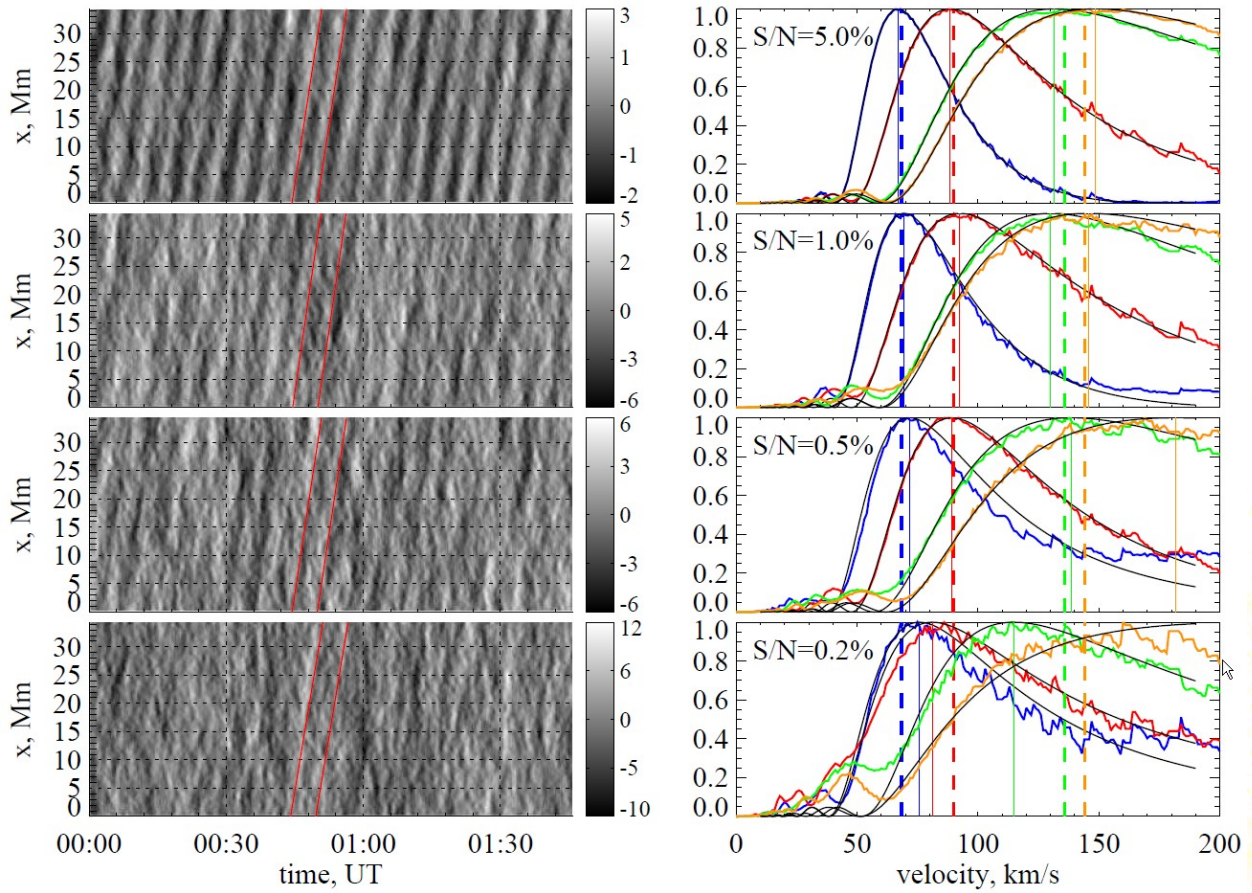

ST analysis of simulated wave signals in four SDO AIA channels. Left: time-differenced position-time plots of a harmonic wave signal in the 171 °A channel. Right: velocity spectrograms obtained for each channel; the phase speed of the wave is adjusted to the temperature the channel assuming that the wave is slow magnetosonic. Color coding: 131 A - blue, 171 A - red, 193 A - green, 211 A - gray. Black curves are least-square fits using the theoretical model (4), solid (dashed) vertical lines are the measured (predicted) propagation velocities for each channel. The amount of additive noise increases from top to bottom as shown by the provided power signal-to-noise ratios (S/N). The tilted red lines on the left panels show the phase speeds and wave periods measured at 171 °A.

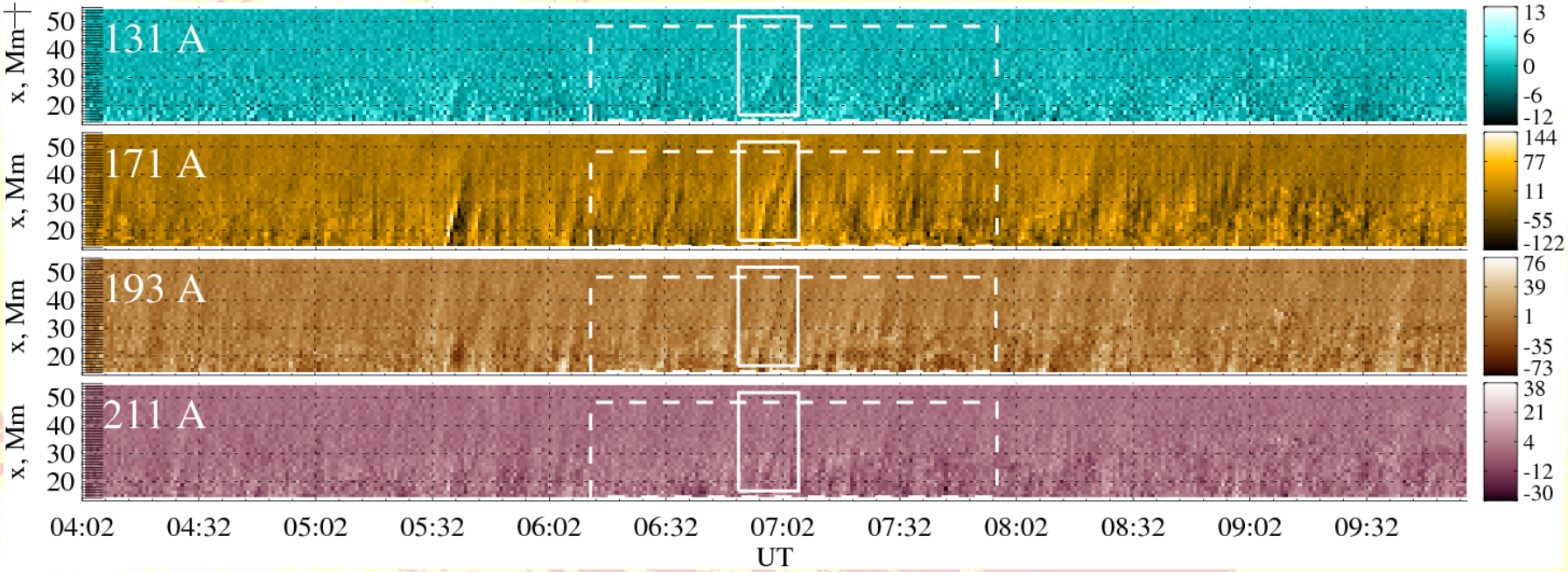
131 A
171 A
193 A
211 A
x, Mm
50
40
30
20
13
6
0
-6
-12
144
77
11
-55
-122
76
39
1
-35
-73
38
21
4
-12
-30
04:02
04:32
05:02
05:32
06:02
06:32
07:02
07:32
08:02
08:32
09:02
09:32
UT

i = 15-19

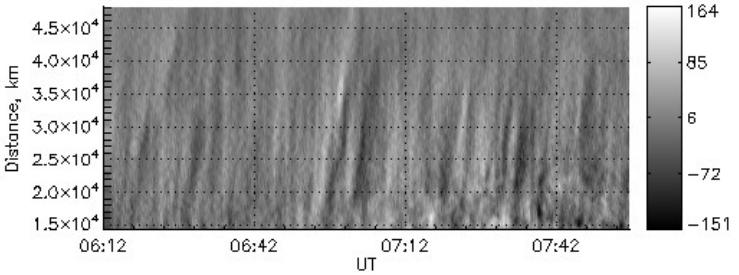
Distance, km
4.5×10^4
4.0×10^4
3.5×10^4
3.0×10^4
2.5×10^4
2.0×10^4
1.5×10^4
06:12
06:42
07:12
07:42
UT
164
85
6
−72
−151

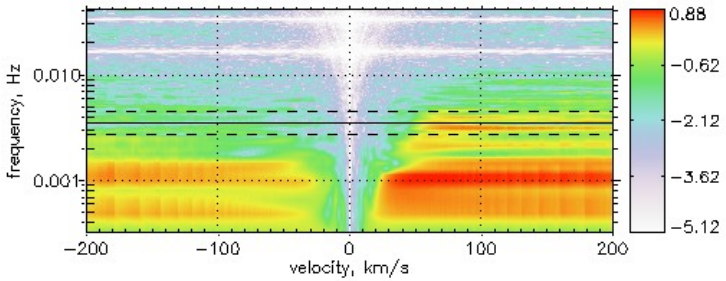
frequency, Hz
0.010
0.001
−200
−100
0
100
200
velocity, km/s
0.88
−0.62
−2.12
−3.62
−5.12

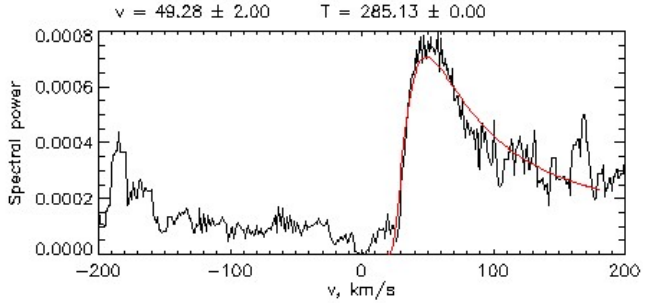
v = 49.28 ± 2.00
T = 285.13 ± 0.00
Spectral power
0.0008
0.0006
0.0004
0.0002
0.0000
−200
−100
0
100
200
v, km/s

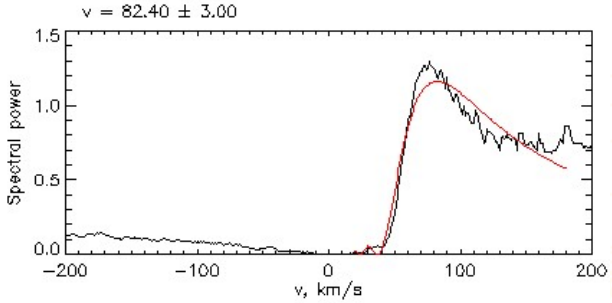
v = 82.40 ± 3.00
Spectral power
1.5
1.0
0.5
0.0
−200
−100
0
100
200
v, km/s

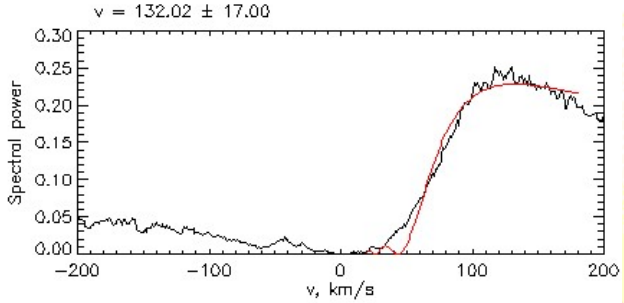
v = 132.02 ± 17.00
Spectral power
0.30
0.25
0.20
0.15
0.10
0.05
0.00
−200
−100
0
100
200
v, km/s

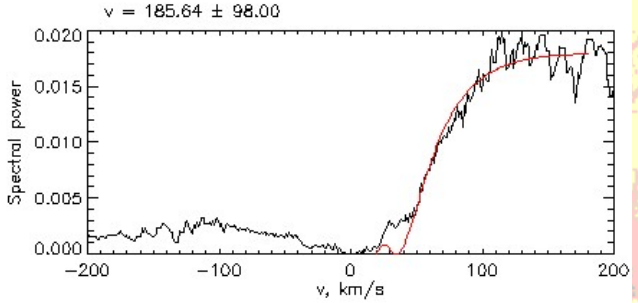
v = 185.64 ± 98.00
Spectral power
0.020
0.015
0.010
0.005
0.000
−200
−100
0
100
200
v, km/s

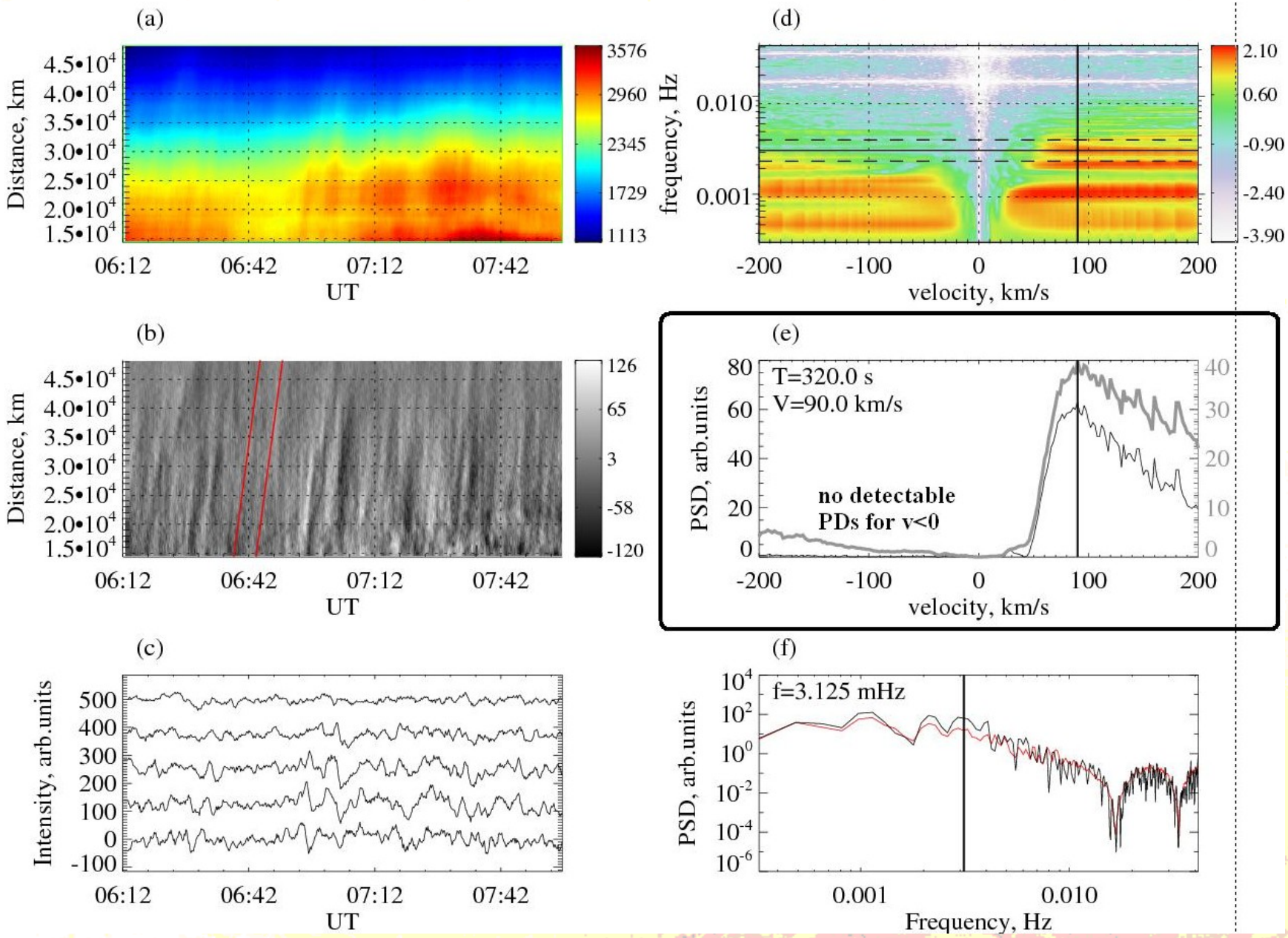
(a)
Distance, km
4.5•10^4
4.0•10^4
3.5•10^4
3.0•10^4
2.5•10^4
2.0•10^4
1.5•10^4
3576
2960
2345
1729
1113
06:12
06:42
07:12
07:42
UT
(b)
Distance, km
126
65
3
-58
-120
UT
(c)
Intensity, arb.units
500
400
300
200
100
0
-100
UT
(d)
frequency, Hz
0.010
0.001
2.10
0.60
-0.90
-2.40
-3.90
-200
-100
0
100
200
velocity, km/s
(e)
PSD, arb.units
80
60
40
20
0
40
30
20
10
0
T=320.0 s
V=90.0 km/s
no detectable
PDs for v<0
velocity, km/s
(f)
PSD, arb.units
10^4
10^2
10^0
10^-2
10^-4
10^-6
f=3.125 mHz
0.001
0.010
Frequency, Hz

#	slices	PD period, s	log f-range	PD velocity, km/s			
				131A	171A	193A	211A
0	0-4	–	–	–	–	–	–
1	5-9	470	1.5	47 ± 3	71 ± 5	83 ± 13	95 ± 4
2	10-14	276	1.5	–	95 ± 4	112 ± 6	–
3	15-19	285	1.3	49 ± 6	82 ± 3	132 ± 17	185 ± 98
4	20-24	344	1.5	–	–	115 ± 14	–
5	25-29	402	1.5	–	100 ± 10	122 ± 14	98 ± 7
6	30-34	456	1.2	–	–	116 ± 10	165 ± 57
7	35-39	–	–	–	–	–	–
8	40-44	415	1.2	64 ± 3	86 ± 3	–	–
9	45-49	276	1.2	–	72 ± 4	95 ± 7	–